Protein Science (1996), 5:2095–2103. Cambridge University Press. Printed in the USA.

NMR characterization of structure, backbone dynamics, and glutathione binding of the human macrophage migration inhibitory factor (MIF)

PETER MÜHLHAHN,[1] JÜRGEN BERNHAGEN,[2] MICHAEL CZISCH,[1] JULIA GEORGESCU,[1] CHRISTIAN RENNER,[1] ALFRED ROSS,[1] RICHARD BUCALA,[3] AND TAD A. HOLAK[1]

[1]Max Planck Institute for Biochemistry, D-82152 Martinsried, Germany
[2]University of Stuttgart, Chair for Interfacial Engineering, Frauenhofer Institute, Nobelstr. 12, D-70569 Stuttgart, Germany
[3]The Picower Institute for Medical Research, 350 Community Drive, Manhasset, NewYork 11030

(RECEIVED June 4, 1996; ACCEPTED July 22, 1996)

Abstract

Human macrophage migration inhibitory factor is a 114 amino acid protein that belongs to the family of immunologic cytokines. Assignments of ^{1}H, ^{15}N, and ^{13}C resonances have enabled the determination of the secondary structure of the protein, which consists of two α-helices (residues 18–31 and 89–72) and a central four-stranded β-sheet. In the β-sheet, two parallel β-sheets are connected in an antiparallel sense. From the total of three cysteines present in the primary structure of MIF, none was found to form disulfide bridges. ^{1}H-^{15}N heteronuclear T_1, T_2, and steady-state NOE measurements indicate that the backbone of MIF exists in a rigid structure of limited conformational flexibility (on the nanosecond to picosecond time scale). Several residues located in the loop regions and at the N termini of two helices exhibit internal motions on the 1–3 ns time scale. The capacity to bind glutathione was investigated by titration of a uniform ^{15}N-labeled sample and led us to conclude that MIF has, at best, very low affinity for glutathione.

Keywords: backbone dynamics; glutathione binding; human macrophage migration inhibitory factor; structure

The cytokine macrophage MIF was originally described 30 years ago as a mediator released by activated T lymphocytes that inhibited the random migration of macrophages in vitro (Bloom & Bennett, 1966; David, 1966). Recent molecular cloning of both human and mouse MIF has made it possible to express and purify recombinant MIF and to produce MIF-specific antibodies that were then used to investigate the specific biological functions of MIF (Weiser et al., 1989; Bernhagen et al., 1993, 1994; Mitchell et al., 1995). This led to a redefinition of MIF as an anterior pituitary hormone, macrophage, and T-cell cytokine, and to its identification as a critical component of the host response to endotoxemia. MIF exists pre-formed in various cell types and tissues and is released specifically in response to a number of inflammatory mediators (Bernhagen et al., 1993, 1996; Galat et al., 1993; Calandra et al., 1994; Nishino et al., 1995). It is the first cytokine to be discovered that is secreted directly from immune cells upon incubation with glucocorticoids, which normally act to suppress immune cell activity. Once released, MIF functions to override the antiinflammatory effects of steroids, thus acting as an endogenous counterregulator of glucocorticoids (Calandra et al., 1995).

Beyond its role as a mediator of the host immune and inflammatory responses to various stress situations, MIF may have functions outside the immune system. Expression of MIF as a growth factor in fibroblasts, its role in early stages of differentiating epithelial cells of the eye lens, and its ability to bind to the interferon antagonist and growth promotor sarcolectin have led to the suggestion that MIF may have a role in cell growth and differentiation (Lanahan et al., 1992; Wistow et al., 1993; Zeng et al., 1993). MIF may exert some of its functions by catalyzing certain enzymatic reactions; it has been proposed that MIF exhibits glutathione-S-transferase (GST) and tautomerase activity (Blocki et al., 1992; Nishihara et al., 1993; Sakai et al., 1994; Rosengren et al., 1996).

In the present article, we describe the determination of the complete secondary structure of huMIF in solution using NMR spectroscopy. ^{15}N NMR relaxation experiments were performed to characterize further MIF protein structure and stability. In addition, we studied the recently postulated capability of MIF to bind GSH (Nishihara et al., 1993).

Reprint requests to: Tad A. Holak, Max Planck Institute for Biochemistry, Am Klopferspitz 18 a, D-82152, Martinsried, Germany; email: holak@genmic.biochem.dpg.de.

Abbreviations: 2D, two-dimensional; 3D, three-dimensional; CBCA(CO)NH, 3D C^{β}-C^{α}-NH correlation spectrum; CT, constant time; D_2O, deuterated water; DTT, dithiothreitol; GSH, reduced glutathione; HNCA, 3D $^{1}H^{N}$-$^{15}N^{H}$-$^{13}C^{\alpha}$ correlation spectrum; HSQC, heteronuclear single quantum coherence spectroscopy; huMIF, human macrophage migration inhibitory factor; IPTG, isopropyl-βD-thiogalactoside; NOE, nuclear Overhauser effect; NOESY, two-dimensional NOE spectroscopy; NMR, nuclear magnetic resonance; TPPI, time proportional phase incrementation.

Results

Backbone assignments

The MIF protein used in this study consists of residues Pro 1–Ala 114 of the huMIF sequence plus an initial methionine residue. Assignment of the backbone ^{1}H, ^{13}C, and ^{15}N resonances was accomplished by use of triple resonance NMR techniques (Bax & Grzesiek, 1993). The ^{1}H–^{15}N HSQC was of good quality and the dispersion of $^{1}H^{N}$–^{15}N amide resonances clearly indicated a folded protein. A total of 124 peaks was found in the HSQC spectrum recorded with presaturation of the water resonance. The HSQC with a WATERGATE sequence for water suppression yielded 129 peaks, with 101 peaks from the backbone NH correlations. The expected number of backbone correlations is 107, so six $^{1}H^{N}$–^{15}N backbone correlations were not found in the HSQC spectrum. The other signals could be assigned to sidechain $^{1}H^{N}$–^{15}N correlations. An example of the $^{1}H^{N}$–^{15}N WATERGATE-HSQC spectrum of MIF is shown in Figure 1.

The 2D ^{1}H TOCSY spectrum of MIF contained only 74 of the excepted 106 H^{N}–H^{α} cross peaks and no cross peaks to β protons or beyond could be found for any residue. This lack of cross peaks in the TOCSY spectrum, together with the observed proton line widths, indicated aggregation or multimerization of the protein. A similar observation was reported by Nihishira et al. (1993), who suggested that MIF existed at least in a dimeric form in solution. The triple-resonance spectra, however, were of good quality. Assignments with $^{13}C/^{15}N$ doubly labeled MIF were based on the following spectra: HNCA (Ikura et al., 1990), CBCA(CO)NH, HNCO (Ikura et al., 1990), HCACO, HCCH-TOCSY (Bax & Grzesiek, 1993). For identification of amino acid types, a HCCH-TOCSY was used. Only few signals of the H and H^{δ} of Ile and Leu residues were observed in the spectrum. Therefore, selective ^{15}N–Ala, ^{15}N–Gly/Ser, and ^{15}N–Ala/Leu labeled samples were prepared to help identify these amino acids. All selectively labeled amino acids were assigned, except Gly 17, Ser 53, Gly 69, and Ala 70, for which no signals could be found in the HSQC and triple resonance spectra at pH 7.0. However, these peaks appeared after lowering pH to 6.5. The $^{13}C^{\alpha}$ and $^{13}C^{O}$ frequencies of seven of the eight proline residues were found in the CBCA(CO)NH and in the HNCO on the NH frequency of the residues (i + 1). A complete list of assignments is given in Table 1 of the Electronic Appendix.

Secondary structure

An overview of the observed medium range backbone NOEs is given in Figure 2. These NOEs are the basis for the determination of the secondary structure elements in proteins (Wüthrich, 1986). A large number of medium-range and long-range NOEs could be identified in the 3D ^{15}N-resolved [^{1}H,^{1}H]-NOESY-HSQC spectra recorded at 29°C. Short distances characteristic of α-helices, comprising $H^{N}(i)$-$H^{N}(i+1)$, $H^{N}(i)$-$H^{N}(i+2)$, $H^{\alpha}(i)$-$H^{N}(i+3)$, and $H^{\alpha}(i)$-$H^{N}(i+4)$, were found in the NOESY spectra. Many interstrand contacts found in β-sheets (Wüthrich, 1986) were also observed. Additionally, chemical shifts of backbone atoms ($^{13}C^{\alpha}$, $^{13}C^{O}$, and $^{1}H^{\alpha}$) were used to predict the type of secondary structure present in the sequence (see the Electronic Appendix) (Spera & Bax, 1991; Wishart et al., 1991). To resolve a few of the overlapping signals in the NH region of the spectra, a 2D HSQC-NOESY (Norwood et al., 1990) of the selective ^{15}N-Ala/Leu-labeled

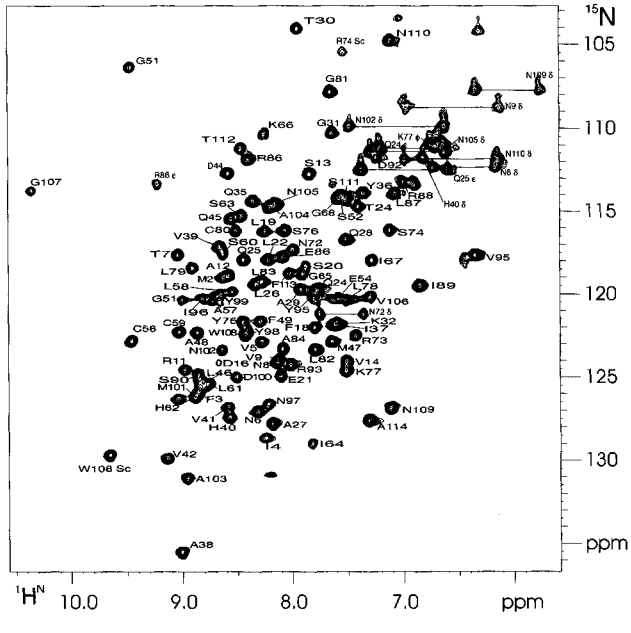

Fig. 1. ^{1}H-^{15}N HSQC spectrum of uniformly ^{15}N-labeled huMIF recorded at pH 7.0, 304 K, and 600 MHz. Residue-specific assignments of the backbone ^{1}H and ^{15}N frequencies are indicated, as is the side chain of the tryptophan residue. The horizontal lines connect the side chain NH_2 frequencies of asparagine and glutamine residues.

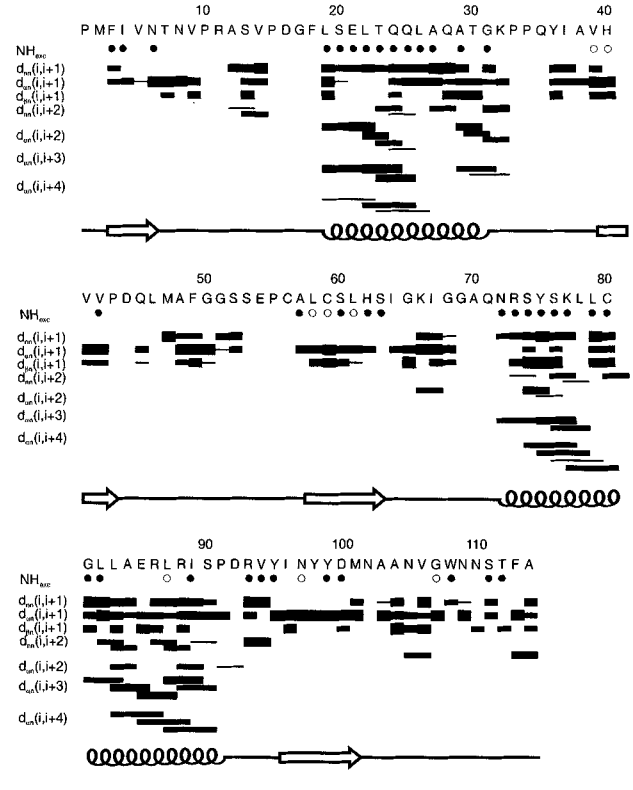

Fig. 2. Schematic representation of the short and medium range NOEs. The NOEs ($i - j < 5$), classified as weak, medium, and strong, are represented by the heights of the bars and were extracted from the ^{1}H-^{15}N-NOESY-HSQC spectra. ●, NHs that did not exchange against D_2O after 5 days; ○, NHs that exchanged after 1 day.

sample was recorded (not shown). In this spectrum the $H^N(i)$-$H^N(i + 1)$ cross peaks between neighboring leucines and alanines in the helices were well separated. The helices are between residues F18 and G31 (helix A) and N72 to I89 (helix B) (Fig. 3). A four stranded β-sheet with a parallel-antiparallel-parallel motif was found between the residues F3–T7, V39–V42, S63–A57, and D100–V94 by identifying the interstrand connectivities shown in Figure 4. Residues F3–T7 and V39–V42 form a parallel β-sheet. Similarly, residues S63–A57 and D100–V94 form another parallel β-sheet. These two parallel β-sheets are joined together in an antiparallel manner. Additionally the C terminus forms an antiparallel β-sheet with a tight turn between residues G107–W108 and S111–T112. Figure 3 shows the topology of the secondary structure elements found in MIF.

^{15}N, T_1, T_2, and HNOE relaxation data

The experimental ^{15}N NOE, T_1, and T_2 values are plotted against amino acid sequence in Figure 5. Accurate peak height measurements for T_1 were possible for 91 resonances from the total of 129 resolved peaks. The mean T_1 was calculated to be 884 ms, ranging from 580 ms for Gln 71 to 995 ms for Thr 7. The mean transverse relaxation time (T_2) of the 94 residues is 49 ms; the maximum value was found for Leu 87, with 62 ms. Quantitative NOE measurements were possible for 78 residues, with an average value of 0.83.

Amide relaxation was analyzed using standard expressions, assuming dipolar coupling between nitrogen and its attached proton and a contribution from the ^{15}N chemical shift anisotropy (Kay et al., 1989; Clore et al., 1990a, 1990b; Stone et al., 1992; Zink et al., 1994). A total of 74 amide protons, for which NOE, T_1, and T_2 could be measured simultaneously, were used in this analysis. The ^{15}N NOE, T_1, and T_2 relaxation data were fit simultaneously to the appropriate expressions of the Lipari-Szabo model (Lipari & Szabo, 1982a, 1982b) using the procedure proposed by Clore et al. (1990b) and Clubb et al. (1995), where S^2, S_S^2, S_f^2, τ_m, τ_e, τ_s, and R_{ex} were used as previously defined (Clore et al., 1990a, 1990b). The overall motion of the protein was assumed to be isotropic. The model of the 3D NMR structure of MIF shows a globular and compact structure for the protein. This preliminary model was based on sequential NOEs (included in this work) and additional intermolecular NOEs that were inconsistent with the determination of a β-strand structure for strand 2, but could be easily explained if MIF was assumed to be a dimer or trimer in solution. The recently published X-ray trimeric structure of MIF from rat liver is in agreement with such a model (Suzuki et al., 1996). The value of τ_m was assessed with two different methods. First, the estimation of τ_m was based on the T_1/T_2 ratio (Kay et al., 1989; Clore et al., 1990a; Clubb et al., 1995; Redfield et al., 1992), resulting in an overall τ_m of 13.3 ns. Another approach used a fixed value for τ_m in each calculation of τ_e and S^2. The calculations were repeated changing τ_m in a range from 3 ns to 20 ns (Zink et al., 1994). The best results with the latter approach were found for a global correlation time of 13.6 ns. Therefore this value was used in the final calculations of the order parameter and internal correlation times.

The specific form of the spectral density function used in the analysis of the relaxation data for a particular residue depended on the value of the T_1/T_2 ratio and the NOE observed experimentally for that residue (Clubb et al., 1995; Redfield et al., 1992; Zink et al, 1994). Selection of the appropriate spectral density was accomplished by initially fitting the data to the simplest spectral density function following the procedure of Clubb et al. (1995). Residues 62, 63, 67, 103, and 111 showed noticeable shortening of T_2 and an average T_1 of 920 ms, slightly longer than the mean T_1 (884 ms) (Fig 5). The relaxation data for these residues could be reproduced using the simplest spectral density function with the addition of the R_{ex} term, which accounts for the effects of chemical exchange line broadening on T_2 (Clore et al., 1990a; Zink et al., 1994). The results of the complete relaxation data analysis are summarized in Figure 6. The data of 52 of 74 measurable backbone amide groups could be accounted for by the simplest spectral density function (Fig. 6).

Glutathione titration experiments

Blocki et al. (1992) proposed that MIF exhibited GST activities. We decided therefore to characterize the affinity of MIF for glutathione by monitoring chemical shifts and line widths of the backbone amide resonances of MIF as a function of the glutathione concentration. To avoid precipitation and large pH changes, two different buffer conditions were used for titration experiments: a high salt buffer with 150 mM Na_2HPO_4/100 mM NaCl, pH 7.0,

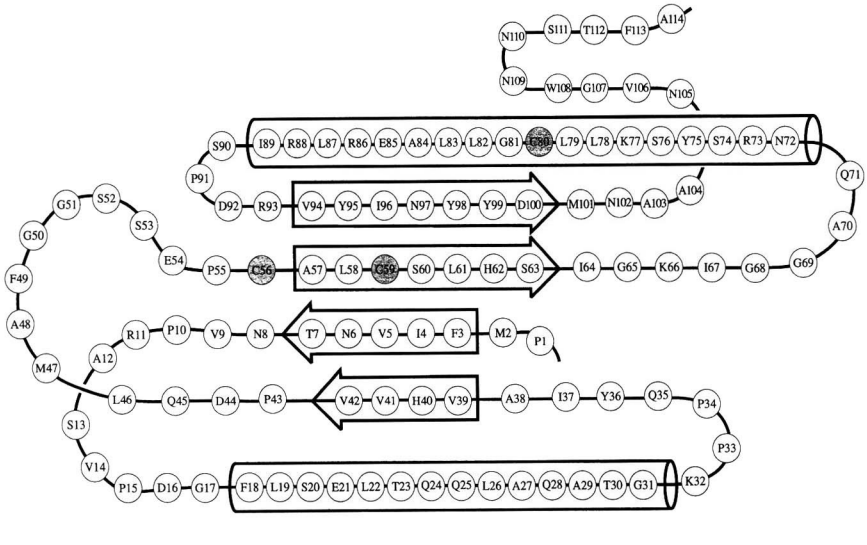

Fig. 3. Schematic diagram of the secondary structure elements in MIF. Numbered circles represent the amino acids in the sequence; cysteines (dark circles) are emphasized. Cylinders indicate the position of α-helices; double-arrowed lines represent β-sheet.

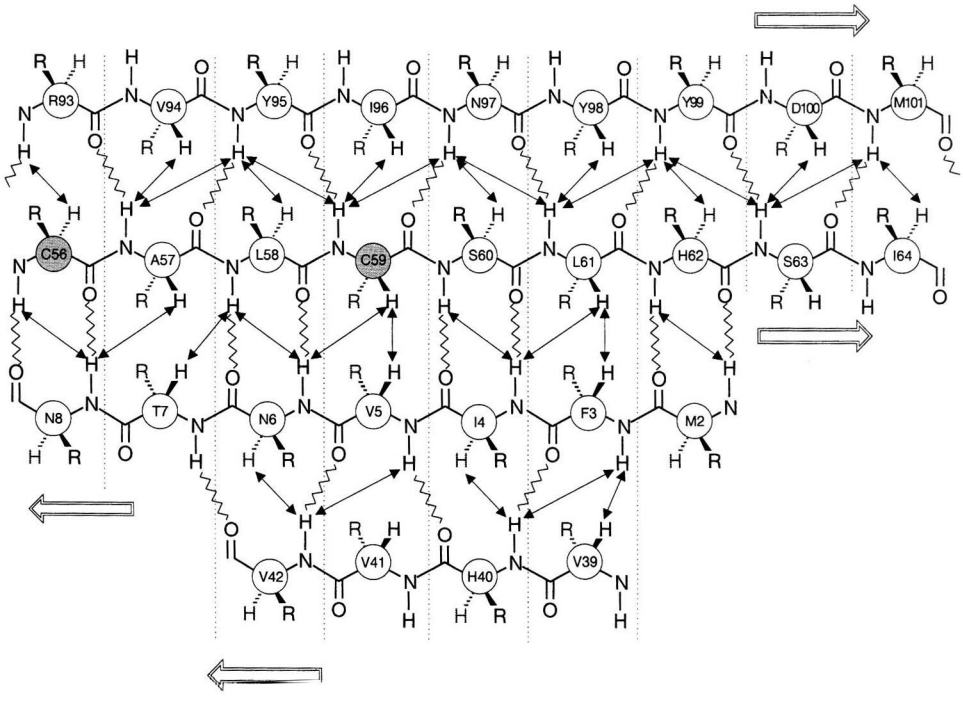

Fig. 4. Diagram of the β-sheet structure of huMIF. Interstrand $H^N(i)$–$H^N(j)$, $H^N(i)$–$H^\alpha(j)$, and $H^\alpha(i)$–$H^\alpha(j)$ NOEs observed in the 3D NOESY-HSQC and 2D NOESY spectra. Zigzag lines represent hydrogen bonds.

and the medium salt buffer with 100 mM K_2HPO_4, pH 6.5. The pH of GSH stock solution was 4.0 for high salt buffer conditions. For the medium salt buffer, the pH of the GSH stock solution was adjusted to 6.5.

Noticeable changes in the chemical shifts during the titration of a 1 mM ^{15}N-labeled sample at the highest salt concentration were observable only after addition of GSH to 8 mM. The final pH of the sample was changed from 7.0 to 6.5. Thus, at this stage it was not possible to determine whether the changes in chemical shifts were due to the binding of MIF to glutathione or to the change in the pH of the sample. Two control experiments were therefore carried out. First, the pH of the GSH-titrated sample was re-adjusted back to pH 7.0. Second, a uniformly ^{15}N-labeled sample was titrated with an acid from pH 7.0 to 6.5. These experiments showed that the same signals were affected both by the GSH titration and acid adjustment. In addition, the magnitude and direction of the chemical shift changes during both experiments were the same. The GSH titration experiment was therefore repeated under the conditions used for the determination of the GSH binding constants by CD spectroscopy (Nishihara et al., 1993), with MIF and the GSH stock solution in the same buffer with a pH of 6.5 (medium salt buffer conditions). The changes of the $^1H^N$ and ^{15}N frequencies were very small and first occurred at a GSH concentration above 8 mM (Fig. 7). The $^1H^N$ and ^{15}N frequencies of the amide side chains changed also only slightly during the titration, with the exception of Trp 108 where the $H^{N\epsilon}$ showed a change of 0.09 ppm ($^1H^N$ frequency) and 0.02 ppm (^{15}N frequency) at concentration of GSH of 16 mM. These results, together with the fact that GSH addition did not affect ^1H and ^{15}N line widths, indicate that MIF has at best very low affinity for glutathione.

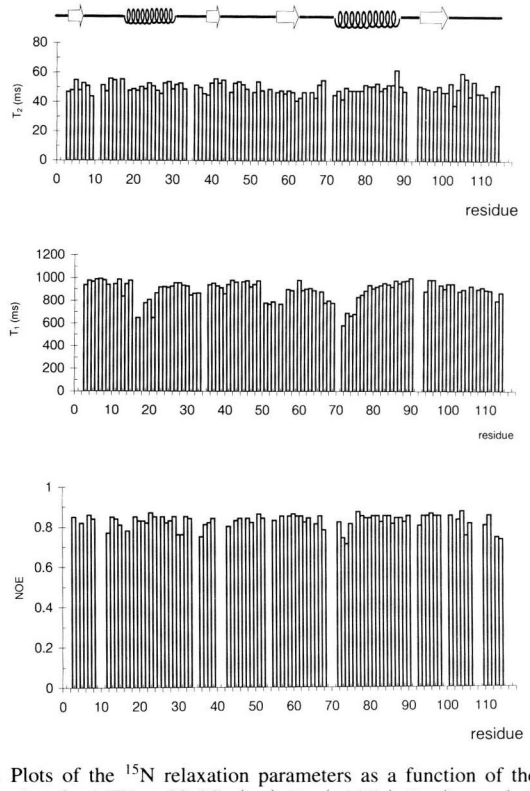

Fig. 5. Plots of the ^{15}N relaxation parameters as a function of the residue number for MIF at 29 °C: (top) T_2, (middle) T_1, (bottom) heteronuclear NOE. Residues for which no results are shown correspond either to proline residues or to residues for which the relaxation data could not be extracted.

Discussion

Initial structural investigations by circular dichroism spectropolarimetry and sequence-based predictions of the secondary structure revealed that MIF belongs to the α/β family of proteins that contain a significant percentage of β-sheet structure and is of medium thermodynamic stability (Bernhagen et al., 1994; Nishihara et al., 1995). These predictions are now confirmed by our present study and by a recent crystal structure of the rat MIF (Suzuki et al., 1996). huMIF consists of two helices between residues Phe 18 and Gly 31 (helix A) and between Asn 72 and Ile 89 (helix B) and a four stranded β-sheet with a parallel-antiparallel-parallel motif, which was found between the residues Phe 3–Thr 7, Val 39–Val 42, Ser 63–Ala 57, and Asp 100–Val 94 (Fig. 4). A comparison of the secondary structure of human and rat MIF showed only two significant differences. β-Strand 39–42 and α-helix 72–89 of huMIF (Fig. 4) are three and four residues longer in the rat MIF structure, residues 36–42 and 68–88, respectively (Suzuki et al., 1996).

Although the analysis of all NOE data is not complete at present, we were able to identify three NOE contacts between the second β-strand and residues Ala 48 and Phe 49 (Ala 48 H^N–Val 39 H^N, Val 39 H^N–Phe 49 H^α, and Phe 49 H^α–Ala 38 H^α). Additionally, signal intensities of sequential NOEs and chemical shift indexes for these residues showed values typical for a β-strand conformation. These results suggest the presence of an antiparallel intermolecular β-sheet seen in the crystal structure (Val 39–Val 42 in one monomer and Leu 46–Ser 50 in the other molecule).

The MIF polypeptide sequence contains three cysteines. Two cysteines (Cys 56 and Cys 59) were suggested to be involved in the disulfide bridge (Bernhagen et al., 1995); the remaining cysteine could be involved in formation of an intermolecular disulfide bridge. In our secondary structure, Cys 56 and Cys 59 are located in the same β-strand 3 and consequently no disulfide bridge is possible. Sulfur atom of Cys 80 is more than 7 Å away from sulfur atoms of Cys 56 and Cys 59 in the trimer crystal structure, indicating that all cysteines are present as free thiols. Supporting evidence for this conclusion is provided by titration of a uniformly ^{15}N-labeled sample with DTT. At the final concentration of DTT 12 mM, there were no significant changes in chemical shifts and line widths. Two control HSQC spectra recorded 1 day and 1 week after the titration also showed no changes in the spectra.

The heteronuclear ^{15}N relaxation data of MIF indicated that most of the protein backbone existed in a rigid structure of limited conformational flexibility (on the nanosecond to picosecond time scale), with any motions faster than τ_m of small magnitude (Lipari & Szabo, 1982a, 1982b; Kay et al., 1989; Clore et al., 1990a, 1990b; Palmer et al., 1991; Barbato et al., 1992; Redfield et al., 1992; Stone et al., 1992; Zink et al., 1994). It is interesting to note that residues located at the N and C termini of the protein were also contained in a well-defined region of the molecule and did not exhibit properties typical for N- or C-terminal residues, which

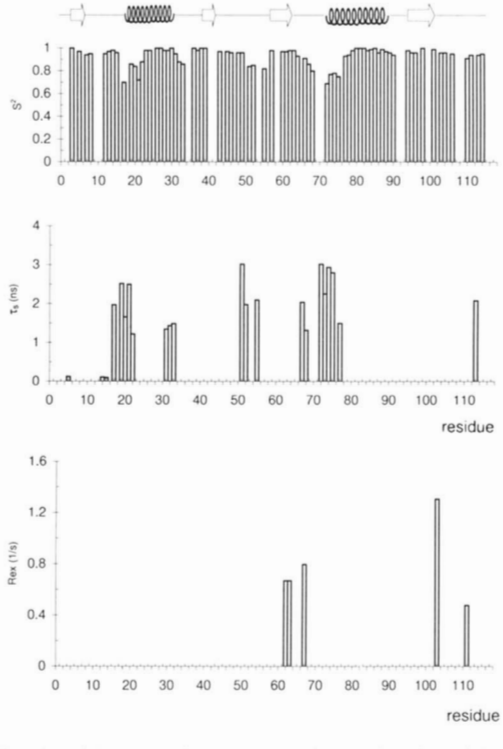

Fig. 6. Results of the relaxation data analysis as a function of the residue number. The generalized order parameter S^2 (top), the effective correlation time τ_s (middle) for the slower internal motion for residues whose relaxation data were fitted to the extended spectral density function (Clore et al., 1990b) and the R_{ex} parameter (bottom) are shown.

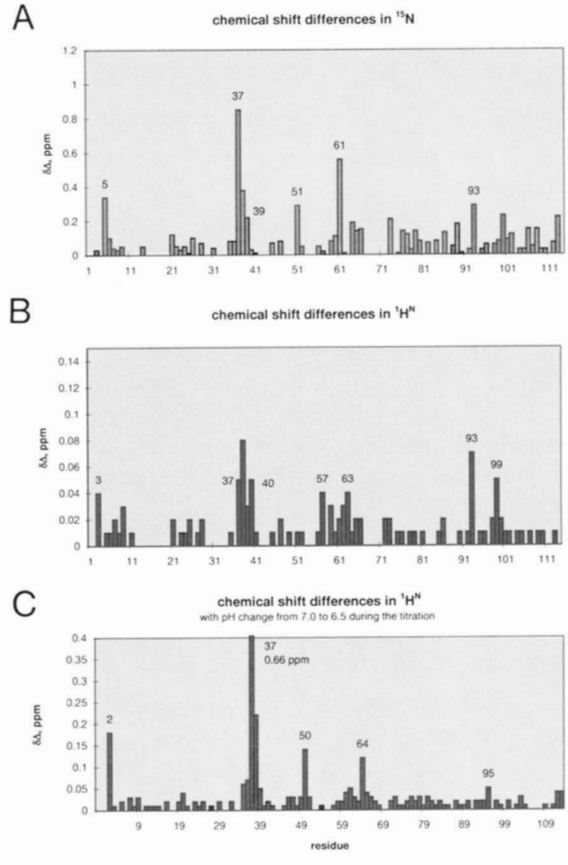

Fig. 7. Change $\delta\Delta$ in the chemical shifts versus amino-acid residue number of huMIF. **A** and **B** indicate the change of the ^{15}N and $^1H^N$ chemical shifts, respectively, during the GSH titration (pH 6.5, the final GSH concentration 16 mM); the protein dissolved in 100 mM K_2HPO_4, pH 6.5. **C** shows the change during the GSH titration (GSH: pH 4.0, the final concentration 16 mM); MIF in the high salt buffer (150 mM Na_2HPO_4/100 mM NaCl, pH 7.0). The final change of pH in the sample from 7.0 to 6.5.

often have increased flexibility. Slow motions (ca. 30 ns to ms) that cause ^{15}N T_2 exchange broadening were observed only for few residues and the magnitude of these processes was relatively small (Fig. 6).

The relaxation data of several residues (Fig. 6) were best interpreted with the extended model-free formalism using S^2, S_S^2, S_f^2, τ_m, τ_e, and τ_s as fit parameters (Clore et al., 1990b). These residues experienced internal motions on a time scale between 1–3 ns (Fig. 6). The simplest physical model for such motions may involve large amplitude jumps between well-defined orientations (Clore et al., 1990a), which, for example, could be stabilized by hydrogen bonds (Chandrasekhar et al., 1992; Eriksson et al., 1993). The residues that experienced these internal motions were located in loops and turns, and at the N termini of two helices present in the secondary structure of the protein. The segment of residues 17–22 and 72–75 encompasses the N terminus of helix 18–35 and helix 72–89, respectively. There was no evident correlation between the presence of these motions and the sensitivity of the residues to changes in the chemical shifts upon lowering pH. The pH sensitive residues were located on one side of the central four-stranded β-sheet (Fig. 7); all these residues are at the monomer–monomer interface of the trimer in the crystal structure. However, other pH sensitive residues possessed relaxation parameters equal to the average value. This was especially true for Ala 38 and Ile 37, which exhibited the largest alteration of chemical shift when the pH changed.

The proton line widths of MIF observed in the NMR spectra were larger than those expected for a protein of 12.5 kDa. Consequently, the proton 2D TOCSY spectra were of poor quality. These observations, together with the global correlation time for the molecular tumbling of the MIF molecule in the range of 13 ns, indicated multimerization of the protein. The τ_m of 13.6 ns would be best in agreement with the dimeric structure of MIF in solution, although trimerization cannot be excluded at present. A similar observation was reported by Nihishira et al. (1993), who suggested that MIF existed at least in a dimeric form in solution based on gel filtration and analytical ultracentrifugation experiments. As previously mentioned, the rat MIF exists as a trimer in the crystal (Suzuki et al., 1996). However, the protein could still be only dimeric in solution because the interface interactions between monomers is not extensive in the crystal structure. The precise determination of the multimerization state of huMIF in solution must await full NMR determination of its three-dimensional structure. This work is now in progress in our laboratory.

It has been proposed that MIF exhibits GST and tautomerase activities (Blocki et al.,1992; Rosengren et al., 1996). Although GST activity of MIF has remained controversial (Pearson et al., 1994), several lines of evidence have suggested that MIF exhibits specific binding affinity for glutathione; for example, a binding constant has been determined to be between 500 and 600 μM (Nishihara et al., 1993; Sakai et al., 1994; Suzuki et al., 1996). Our GSH titration experiments, performed under the conditions used for the determination of the GSH binding constants by CD spectroscopy (Nishihara et al., 1993), indicate that MIF has very low, if any, affinity for glutathione.

Materials and methods

Materials

^{15}N-ammonium chloride, ^{13}C-glucose, and ^{15}N-labeled leucine, glycine, and alanine were purchased from Campro, Veenendaal, The Netherlands, and D_2O from Cambridge Isotope Laboratories. Bacto-agar and Bacto-yeast extract were purchased from Difco Laboratories (Detroit, MI). All other chemicals were from Merck (Darmstadt, Germany).

Sample preparation

For the preparation of all MIF samples for our NMR studies, a pET11b vector transformed in the *Escherichia coli* BL21(DE3) expression strain was used and the protein obtained by overproduction was purified as described elsewhere (Bernhagen et al., 1994).

The uniformly ^{15}N-labeled and the $^{13}C/^{15}N$-double-labeled samples were prepared by growing the bacteria on M9 minimal medium containing ^{15}N-ammonium chloride (1 g/L) as the only nitrogen source (Sambrook et al., 1989), or ^{15}N-ammonium chloride (1 g/L) and ^{13}C-glucose (2 g/L) in case of double-labeled samples, supplemented with minerals and cofactors (Hoffman & Spicer, 1991). For selective labeled samples, the minimal medium consisted of the isotopically enriched amino acid and all other unenriched amino acids, except for the ^{15}N-Gly/^{15}N-Ser labeled sample, which contained no serine (Muchmore et al., 1989). The ^{15}N-Gly/^{15}N-Ser [^{15}N-glycine (1 g/L)] sample, ^{15}N-alanine–labeled sample [^{15}N-alanine (800 mg/L)], ^{15}N-Ala/^{15}N-Leu [^{15}N-alanine (800 mg/L)], and ^{15}N-leucine (300 mg/L) were prepared in this manner. Two liters of the corresponding medium, containing carbenicillin (50 μg/mL), were inoculated from a 20 mL overnight culture and grown at 37 °C to an optical density at 600 nm of 0.7. IPTG was added to final concentrations of 1 mM and the bacteria were shaken another 4 hours before being harvested by centrifugation. The protein was isolated (after disruptions of the cells with glass beads) by FPLC anion exchange chromatography (MonoQ HR10/10 Pharmacia, bed volume 10 mL). To obtain essentially purified samples, a reverse phase chromatography followed.

Samples for NMR typically contained 1–2 mM protein dissolved in 20 mM Na_2HPO_4, 0.5 mM EDTA, 0.02% NaN_3, and 90% H_2O/10% D_2O, pH 7.0. For recording spectra in D_2O, the samples were concentrated with Centricon 10 and dissolved in 100% D_2O buffer.

NMR spectroscopy

All NMR experiments were carried out at 304 K on a Bruker DRX600 spectrometer and a Bruker AMX500 spectrometer. The DRX600 spectrometer was equipped with a triple resonance probehead and PFG accessories (BGU-II Z gradient system).

The 2D TOCSY was performed according to the method of Rance with the MLEV-17 sequence (Bax & Davis, 1985) for isotropic mixing and spin-lock periods of 10, 20, and 40 ms. The TOCSY pulse sequences included presaturation of the water resonance for measurements in H_2O (Guèron et al., 1991). NOESY experiments (Jeener et al., 1979) were recorded with a pulse sequence in which the last 90 degree pulse was replaced by a jump-return sequence to suppress the water resonance (Plateau & Guèron, 1982). A homospoil pulse of 8 ms during the mixing time of 100 ms was also used. A total of 2,048 complex data points were acquired in the time domain t_2 with a spectral width of 11.73 ppm in the F_2 dimension; 800 increments in the time period t_1 with an F_1 spectral width of 11.73 ppm and 96 scans per t_1 value were added. Quadrature detection in the indirectly detected dimensions was obtained with the TPPI method (Marion & Wüthrich, 1983).

The 2D ^1H-^{15}N HSQC correlation spectra were recorded as described by Mori et al. (1995) to avoid signal losses due to fast chemical exchange. The resonances of the NH_2 side chains were

identified using heteronuclear triple quantum coherence (Schmidt & Rüterjans, 1990). For all ^1H-^{15}N correlations, 150 t_1 increments were acquired with a sweep width of 2,500 Hz in the nitrogen dimension. The 3D ^1H-^{15}N-NOESY-HSQC spectrum (Jahnke et al., 1995a) was recorded with a mixing time of 100 ms, and with 32 scans per t_1-t_2 pair. The spectral width and number of points acquired were 11.57 ppm and 90 complex points in $^1H(F_1)$, 44.11 ppm and 22 complex points in $^{15}N(F_2)$, and 5.24 ppm and 1,024 complex points in $^1H(F_3)$ with the $^1H(F_1)$, $^{15}N(F_2)$, and $^1H^N(F_3)$ carrier frequencies placed at 4.73 ppm, 109.82 ppm, and 4.73 ppm, respectively.

Sequential assignment was performed with triple-resonance experiments. The sequences that start with the NH magnetization were performed in such a way as to avoid signal losses due to chemical exchange. Modified versions of the CT-HNCA and CT-HNCO experiments (Grzesiek & Bax, 1992), similar to the sequences proposed by Jahnke & Kessler (1995b), were acquired. The HNCA (as well as the 3D NOESY) was run in a sensitivity enhanced version (Palmer et al., 1992). Because these spectra only showed a minor enhancement of approximately 1.1, all other spectra were acquired in the nonenhanced version.

The distinction between intra- and interresidual contacts in the HNCA was achieved with a CBCA(CO)NH (Grzesiek & Bax, 1993). H^α resonances were determined with a HCACO experiment (Powers et al., 1991), run in a gradient enhanced version to allow measurement in water. Finally, side chains were assigned using a gradient enhanced version of the HCCH-TOCSY, as proposed by Kay et al. (1993).

All 3D spectra were processed on a CONVEX 220 with the software CC-NMR (Cieslar et al., 1993). A single zero filling with extensive linear prediction methods in all indirectly detected dimensions was performed. After the peak-picking routine the assignment was performed both manually and by use of program ALFA (Bernstein et al., 1993).

The heteronuclear ^{15}N T_2, T_1, and NOE relaxation measurements of the backbone amides

To avoid problems associated with fast exchanging amide protons, pulse sequences proposed by Farrow et al. (1994) were used. The experiments were not run in a sensitivity enhanced fashion, which made the application of an additional selective pulse on water necessary in the T_1 and T_2 measurements. Suppression of the strong solvent signal was achieved with a WATERGATE sequence (Sklenář et al., 1993) instead of a coherence selection of the original pulse sequence (Farrow et al., 1994). For the T_1 measurements, the relaxation delay consisted of two 180 degree refocussing pulses on ^1H with a phase difference of 180 degrees. Cumulative effects on the water resonance (due to the pulse angle imperfections) were therefore reduced. T_1 data points were obtained with nine spectra in which the relaxation period of 11 ms were repeated: n = 1, 4, 8, 16, 32, 64, 128, 170, and again 1 time within the relaxation delay. The transverse relaxation time was sampled at ten points: n = 1, 2, 3, 4, 5, 6, 8, 10, 1, and 4, with a basic CPMG block of 14.3 ms. Saturation of the amide protons in the heteronuclear NOE experiment was achieved by the application of a series of 120 degree pulses prior to the experiment (Farrow et al., 1994).

Extraction of the T_1, T_2 times and NOEs

Intensities of the cross peaks in the T_1, T_2, and NOE spectra were obtained from the peak heights. T_1 and T_2 were calculated by fitting the function $[a \times \exp(t/T_{1,2})]$ to the data values. To minimize the mean square differences between the experimental intensities d_i and the fit function $\{E[T_{1,2}] = \sum[d_i - a \times exp(t_i/T_{1,2})]^2\}$, T was scanned in 400 equal steps in a time range of 20 to 1,000 ms. Uncertainties in the calculated relaxation times were determined in an analogous manner to that described by Stone et al. (1992) and Zink et al. (1994). The $1/T_1$ and $1/T_2$ rates used in the present study are those for which the standard deviations to the fitted $1/T_1$ and $1/T_2$ values were less than 10%.

Glutathione titration

Glutathione titration of MIF was initially performed with a uniformly ^{15}N-labeled sample with a protein concentration of ca. 1 mM in a high salt buffer containing 150 mM Na_2HPO_4, 100 mM NaCl, 0.5 mM EDTA, 0.02% NaN_3, 90% H_2O/10% D_2O, pH 7.0. The titration was done first in steps of 1 mM and later in steps of 2 mM of GSH, with a final glutathione concentration of 16 mM. GSH, as delivered from the manufacturer, had pH 4 when dissolved in pure water. It was thought that addition of minute amounts of GSH to a buffered high salt solution of the protein would not change the pH of the protein solution. This proved not to be the case: a 0.5 drop in pH was observed. Thus, it was not possible to determine from this experiment whether the changes in chemical shifts were due to the binding of MIF to glutathione or to the change in the pH of the sample. In the end, however, this experiment was valuable because it showed an important property of MIF: high sensitivity of NMR resonances for certain residues to even slight changes in pH.

The second titration was performed for the MIF sample dissolved in 100 mM K_2HPO_4, pH 6.5. The GSH stock solution was also prepared in the same buffer and pH of 6.5. These conditions were similar to those used in the determination of the GSH binding constants by CD spectroscopy (100 mM K_2HPO_4, 0.5 mM EDTA, 0.02% NaN_3, pH 6.5) (Nishihara et al., 1993). In all glutathione titration experiments, a set of HSQC spectra was recorded on a Bruker DRX 600 spectrometer with 128 × 1,024 complex points and eight scans.

DTT titration

A 1 mM uniformly ^{15}N-labeled sample of MIF in 20 mM Na_2HPO_4 buffer at pH 7.0 was used for titration with DTT. The DTT stock solution had pH 7.0. The titration steps were 2 mM DTT, up to a final concentration of 20 mM. Between every single step, a HSQC spectrum was recorded with 128 × 1,024 complex points and eight scans.

Note added in proof

The X-ray structure of human MIF has been recently published: Sun H-W, Bernhagen J, Bucala R, Lolis E, 1996. Crystal structure at 2.6 Å resolution of human macrophage migration inhibitory factor. *Proc Natl Acad Sci USA 93*:5191–5196.

Supplementary material

Supplementary material in the Electronic Appendix consists of Table 1 with the ^1H, ^{13}C, and ^{15}N chemical shifts of the backbone atoms of huMIF and a figure showing the deviation of the chemical shifts relative the random coil values.

Acknowledgments

We thank Tim Mather for stimulating discussions. This work was supported by the Deutsche Forschungsgemeinschaft (Projects B11, Sonderforschungbereich 266 of the Technical University of Munich).

References

Barbato G, Ikura M, Kay LE, Pastor RW, Bax A. 1992. Backbone dynamics of calmodulin studied by ^{15}N relaxation using inverse detected two-dimensional NMR spectroscopy: The central helix is flexible. *Biochemistry 31*:5269–5278.

Bax A, Davis DG. 1985. MLEV-17-based two-dimensional homonuclear magnetization transfer spectroscopy. *J Magn Reson 65*:355–360.

Bax A, Grzesiek S. 1993. Methodological advances in protein NMR. *Acc Chem Res 26*:131–138.

Bernhagen J, Bacher M, Calandra T, Metz CN, Doty S, Donnelly T, Bucala R. 1996. An essential role for macrophage migration inhibitory factor (MIF) in the delayed-type hypersensitivity reaction. *J Exp Med 183*:277–282.

Bernhagen J, Calandra T, Mitchell RA, Martin SB, Tracey KJ, Voelter W, Manogue KR, Cerami A, Bucala R. 1993. MIF is a pituitary-derived cytokine that potentiates endotoxemia. *Nature 365*:756–759.

Bernhagen J, Kapurniotu A, Stoeva S, Voelter W, Bucala. 1995. Conformational and disulfide bond analysis of macrophage migration inhibitory factor (MIF). *Peptides 1994*:572–573.

Bernhagen J, Mitchell RA, Calandra T, Voelter W, Cerami A, Bucala R. 1994. Purification, bioactivity, and secondary structure analysis of mouse and human macrophage migration inhibitory factor (MIF). *Biochemistry 33*: 14144–14155.

Bernstein R, Cieslar C, Ross A, Oschkinat H, Freund J, Holak TA. 1993. Computer-assisted assignment of multidimensional NMR spectra of proteins: Application to 3D NOESY-HMQC and TOCSY-HMQC spectra. *J Biol NMR 3*:245–251.

Blocki FA, Schlievert PM, Wackett LP. 1992. Rat liver protein linking chemical and immunological detoxification systems. *Nature 360*:269–270.

Bloom BR, Bennett B. 1966. Mechanism of a reaction in vitro associated with delayed-type hypersensitivity. *Science 153*:80–82.

Calandra T, Bernhagen J, Metz CN, Spiegel L, Bacher M, Donnelly T, Cerami A, Bucala R. 1995. MIF as a glucocorticoid-induced modulator of cytokine production. *Nature 377*:68–71.

Calandra T, Bernhagen J, Mitchell RA, Bucala R. 1994. The macrophage is an important and previously unrecognized source of macrophage migration inhibitory factor. *J Exp Med 179*:1895–1902.

Chandrasekhar I, Clore GM, Szabo A, Gronenborn AM, Brooks BR. 1992. A 500 ps molecular dynamics of interleukin-1β using two-dimensional inverse detected heteronuclear ^{15}N-^{1}H spectroscopy. *Biochemistry 29*:321–338.

Cieslar C, Ross A, Zink T, Holak TA. 1993. Efficiency in multidimensional NMR by optimized recording of time point-phase pairs in evolution periods and their selective linear transformation. *J Magn Reson Series B 101*:97–101.

Clore GM, Driscoll PC, Wingfield PT, Gronenborn AM. 1990a. Analysis of the backbone dynamics of interleukin 1β using two-dimensional inverse detected heteronuclear ^{15}N-^{1}H NMR spectroscopy. *Biochemistry 27*:7387–7401.

Clore GM, Szabo A, Bax A, Kay LE, Driscoll PC, Gronenborn AM. 1990b. Deviations from the simple two-parameter model-free approach to the interpretation of nitrogen-15 nuclear magnetic relaxation of proteins. *J Am Chem Soc 112*:4989–4991.

Clubb RT, Omichinski JG, Sakaguchi K, Appella E, Gronenborn AM, Clore GM. 1995. Backbone dynamics of the oligomerization domain of p53 determined from ^{15}N NMR relaxation measurements. *Protein Sci 3*:855–862.

David J. 1966. Delayed hypersensitivity in vitro: Its mediation by cell-free substances formed by lymphoid cell-antigen interaction. *Proc Natl Acad Sci USA 56*:72–77.

Eriksson MAL, Berglund H, Härd T, Nilsson L. 1993. A comparison of ^{15}N NMR relaxation measurements with a molecular dynamics simulation: Backbone dynamics of the glucocorticoid receptor DNA-binding domain. *Proteins Struct Funct Genet 17*:375–390.

Farrow NA, Muhandiram R, Singer AU, Pascal SM, Kay CM, Gish G, Shoelson SE, Pawson T, Foreman-Kay JD, Kay LE. 1994. Backbone dynamics of a free and a phosphopeptide-complexed Src homology 2 domain studied by ^{15}N NMR relaxation. *Biochemistry 33*:5984–6003.

Galat A, Riviere S, Bouet F. 1993. Purification of macrophage migration inhibitory factor (MIF) from bovine brain cytosol. *FEBS Lett 319*:233–236.

Grzesiek S, Bax A. 1992. Improved 3D triple-resonance NMR techniques applied to a 31 kDa protein. *J Magn Reson 96*:432–440.

Grzesiek S, Bax A. 1993. Amino acid type determination in the sequential assignment procedure of uniformly $^{13}C/^{15}N$-enriched proteins. *J Biomol NMR 3*:185–204.

Guèron M, Plateau P, Decorps M. 1991. Solvent signal suppression in NMR. *Prog NMR Spectrosc 23*:135–209.

Hoffman DW, Spicer LD. 1991. Isotopic labeling of specific amino acid types as an aid to NMR spectrum assignment of the methione repressor protein. In: Villafranca JJ, ed. *Techniques in protein chemistry II*. San Diego: Academic Press. pp 409–419.

Ikura M, Kay LE, Bax A. 1990. A novel approach for sequential assignment of ^{1}H, ^{13}C and ^{15}N spectra of larger proteins. Heteronuclear triple resonance three dimensional NMR spectroscopy: Application to calmodulin. *Biochemistry 29*:4659–4667.

Jahnke W, Baur M, Gemmecker G, Kessler H. 1995a. Improved accuracy of NMR structures by a modified NOESY-HSQC experiment. *J Magn Reson B106*:86–88.

Jahnke W, Kessler H. 1995b. Modified triple-resonance NMR experiments with optimized sensitivity for rapidly exchanging protons. *Angew Chem Int Ed Engl 34,4*:469–471.

Jeener J, Meier BH, Bachman P, Ernst RR. 1979. Investigation of exchange processes by two-dimensional NMR spectroscopy. *J Chem Phys 71*:4546–4553.

Kay LE, Torchia DA, Bax A. 1989. Backbone dynamics of proteins as studied by ^{15}N inverse detected heteronuclear NMR spectroscopy: Application to staphylococcal nuclease. *Biochemistry 28*:8972–8979.

Kay LE, Xu G-Y, Singer AU, Muhandiram DR, Foreman-Kay JD. 1993. A gradient-enhanced HCCH-TOCSY experiment for recording side-chain ^{1}H and ^{13}C correlations in H_2O samples of proteins. *J Magn Reson B101*:333–337.

Lanahan A, Williams JB, Sanders LK, Nathans D. 1992. Growth factor-induced delayed early response genes. *Mol Cell Biol 12*:3919–3929.

Lipari G, Szabo A. 1982a. Model-free approach to the interpretation of nuclear magnetic resonance relaxation in macromolecules. 1. Theory and range of validity. *J Am Chem Soc 104*:4546–4559.

Lipari G, Szabo A. 1982b. Model-free approach to the interpretation of nuclear magnetic resonance relaxation in macromolecules. 2. Analysis of experimental results. *J Am Chem Soc 104*:4559–4570.

Marion D, Wüthrich K. 1983. Application of phase sensitive two dimensional correlated spectroscopy (COSY) for measurements of ^{1}H-^{1}H spin-spin coupling constants in proteins. *Biochem Biophys Res Commun 113*:967–974.

Mitchell RA, Bacher M, Bernhagen J, Pushkarskaya T, Seldin M, Bucala R. 1995. Cloning and characterization of the gene for mouse MIF. *J Immunol 154*:3863–3870.

Mori S, Abeygunawardana C, Johnson MN, van Zijl PCM. 1995. Improved sensitivity of HSQC spectra of exchanging protons at short interscan delays using a new fast HSQC (FHSQC) detection scheme that avoids water saturation. *J Magn Reson B108*:94–98.

Muchmore DC, McIntosh LP, Russell CB, Anderson DE, Dahlquist FW. 1989. Expression and nitrogen-15 labeling of proteins for proton and nitrogen-15 nuclear magnetic resonance. *Methods in Enzymology 177*:44–73.

Nishihara J, Kuriyama T, Nishino H, Ishibashi T, Sakai M, Nishi S. 1993. Purification and characterization of human macrophage migration inhibitory factor: Evidence for specific binding to glutathione and formation of subunit structure. *Biochem Mol Biol Internat 31*:841–850.

Nishihara J, Kuriyama T, Sakai M, Nishi S, Ohki S-Y, Hikichi K. 1995. The structure and physicochemical properties of rat liver macrophage migration inhibitory factor. *Biochim Biophys Acta 1247*:159–162.

Nishino T, Bernhagen J, Shiiki H, Calandra T, Dohi K, Bucala R. 1995. Localization of macrophage migration inhibitory factor (MIF) to secretory granules within the corticotrophic and thyrotrophic cells of the pituitary gland. *Mol Medicine 1*:781–788.

Norwood TJ, Boyd J, Heritage JE, Soffe N, Campbell ID. 1990. Comparison of techniques for ^{1}H-detected heteronuclear ^{1}H-^{15}N spectroscopy. *J Mag Reson 87*:488–501.

Palmer AG, Cavanagh J, Byrd RA, Rance M. 1992. Sensitivity improvement in three-dimensional heteronuclear correlation NMR spectroscopy. *J Magn Reson 96*:415–424.

Pearson WR. 1994. MIF proteins are not glutathione transferase homologs. *Protein Sci 3*: 525–527.

Plateau P, Guèron M. 1982. Exchangeable proton NMR without base-line distortion using new strong-pulse sequences. *J Am Chem Soc 104*:7310–7311.

Powers R, Gronenborn AM, Clore GM, Bax A. 1991. Three-dimensional triple-resonance NMR of $^{13}C/^{15}N$-enriched proteins using constant-time evolution. *J Magn Reson 94*:209–213.

Redfield C, Boyd J, Smith LJ, Smith RAG, Dobson CM. 1992. Loop mobility in a four-helix-bundle protein: ^{15}N NMR relaxation measurement on human interleukin-4. *Biochemistry 31*:10431–10437.

Rosengren E, Bucala R, Åman P, Jacobsson L, Odh G, Metz CN, Rorsman H.

1996. The immunoregulatory mediator macrophage migration inhibitory factor (MIF) catalyzes a tautomerization reaction. *Mol Medicine 2*:143–149.

Sakai M, Nishihira J, Hibiya Y, Koyama Y, Nishi S. 1994. Glutathione binding rat-liver 13K protein is the homolog of the macrophage-migration inhibitory factor. *Bio Mol Biol Int 33*:439–446.

Sambrook J, Fritsch EF, Maniatis T. 1989. *Molecular cloning: A laboratory manual*, 2nd ed. Cold Spring Harbor, NY: Cold Spring Harbor Laboratory Press.

Schmidt JM, Rüterjans H. 1990. Proton-detected 2D heteronuclear shift correlation via multiple-quantum coherences of the type I_2S. *J Am Chem Soc 112*:1280–1281.

Sklenář V, Piotto M, Leppik R, Saudek V. 1993. Gradient-tailored water suppression for ^1H-^{15}N HSQC experiments optimized to retain full sensitivity. *J Magn Reson A102*:241–245.

Spera S, Bax A. 1991. Empirical correlation between protein backbone conformation and Cα and Cβ ^{13}C nuclear magnetic resonance chemical shifts. *J Am Chem Soc 113*:5490–5492.

Stone MJ, Fairbrother WJ, Palmer AG III, Reizer J, Saier MH, Wright PE. 1992. Backbone dynamics of the *Bacillus subtilis* glucose permease IIA domain determined from ^{15}N NMR relaxation measurements. *Biochemistry 31*:4394–4406.

Suzuki M, Sugimoto H, Nakagawa A, Tanaka I, Nishihira J, Sakai M. 1996. Crystal structure of the macrophage migration inhibitory factor from rat liver. *Nature Struct Biol 3*:259–265.

Weiser WY, Temple PA, Witek-Gianotti JS, Rembold HG, Clark SC, David JR. 1989. Molecular cloning of the cDNA encoding a human macrophage migration inhibitory factor. *Proc Natl Acad Sci USA 86*:7522–7531.

Wishart DS, Sykes BD, Richards FM. 1991. Relationship between nuclear magnetic resonance chemical shift and protein secondary structure. *J Mol Biol 222*:311–333.

Wistow GJ, Shaughnessy MP, Lee DC, Hodin J, Zelenka. 1993. A macrophage migration inhibitory factor is expressed in the differentiating cells of the eye lens. *Proc Natl Acad Sci USA 90*:1272–1280.

Wüthrich K. 1986. *NMR of proteins and nucleic acids*. New York: Wiley.

Zeng FY, Weiser WY, Kratzin H, Stahl B, Karas M, Gabius HJ. 1993. The major binding-protein of the interferon antagonist sarcolectin in human placenta is a macrophage-migration inhibitory factor. *Archiv Bioch Biophys 303*: 74–80.

Zink T, Ross A, Lüers K, Cieslar C, Rudolph R, Holak TA. 1994. Structure and dynamics of the human granulocyte colony-stimulating factor determined by NMR spectroscopy. Loop mobility in a four-helix-bundle protein. *Biochemistry 33*:8453–8463.